

iCRAG Technology Services

University College Dublin
Belfield
Dublin 4

Project: S0002, April 2019

By: Sean Johnson FGS, P.Geo & Pearce
Kavanagh BSc Hon

AIMS

To determine the chemistry and paragenesis of sulfide phases from surface samples at the Gortdrum Cu deposit.

SUMMARY

- Gold is present in low amounts in chalcopyrite in each sample analysed.
- Chalcopyrite hosts most of the trace elements analysed in abundance.
- Samples – 50 and -59a contained 2 texturally diverse Arsenopyrite/ As-bearing pyrite (*sensu stricto*). Gold and precious metal content was low or below detection limit in these phases.
- The two As-pyrite types contained similar trace element content suggesting that though textually different they likely represent similar fluid origins.
- High Co vs Ni ratios along with elevated As, Te and Sb suggest that these As-pyrites are more reflective of a distinct hydrothermal signature, or different pulse of mineralization.
- Pyrite has very few trace elements in notable concentrations.
- Supergene covellite occurring on rims and cracks appears to have re distributed and concentrated Bi and Ag.
- The filtered data are presented in an excel spreadsheet (Appendix 1).

METHODOLOGY

Twelve samples from spoil heaps derived directly from the Gortdrum deposit were received by iCRAG from Group Eleven Resources.

The samples were inspected and areas of interest were selected (based on texture, mineralogy, and alteration). These areas were then cut and mounted in 25 mm round epoxy blocks and polished. These were then inspected in order to provide a brief synopsis of the mineralogical associations within the sample. Unfortunately some samples had pervasive alteration and oxidation to the point where sulphides were no longer present or would be compromised for analysis. Samples were then analyzed for trace elements at the iCRAG

Analytical Facility. A Photon Machines ANALYTE G2 193 nm excimer laser ablation system coupled with a ThermoFisher iCAP Q- ICP-MS was used for all analyses (Analytical parameters are summarized in Table 1). A range of elements were analysed: Mn, Fe, Co, Ni, Cu, Zn, As, Se, Mo, Ag, Cd, Sn, Sb, Te, W, Au, Tl, Pb and Bi. For quantification Fe was used as the internal standard element.

N.B. Fe and S are not reported as they are used in the internal standard and reduction calculations.

For each analysis a background signal was recorded, then after 30 seconds the laser was turned on, the sample was ablated and the ICP-MS collected data for each element (Fig. 1). Some elements are incorporated into the mineral structure and show no or gradual change (zonation). However, evenly distributed invisible micro-inclusions may also show no or gradual change in the signal, but are indistinguishable from zonation with this technique. Elements present in the structure or in micro-inclusions are referred to as refractory. Other elements are concentrated in inclusions and expressed as discrete, sharp changes in the signal. To calculate concentration, the signal was integrated over the time interval shown and calibrated against reference standards.

The element concentrations of all individual analyses are presented in a separate spread sheet, attached, along with average concentrations in each mineral and individual concentrations to a 2 sigma precision. When concentrations were <DL, the DL was used for calculating the average concentration and for plotting. The following report details the distribution of trace elements in the sulphides analysed, with example laser ablation signal plots.

ICP-MS	ThermoFisher iCAP ICP-MS
Laser Ablation Microprobe	Photon ANALYTE G2
Laser wavelength	193 nm
Ablation cell	HeLEX II
Laser Type	Excimer ArF
Fluence	1.5 J/cm ²
Repetition rate	5 Hz
Beam size	30 μm
Data acquisition mode	time resolved
Background acquisition	30 s
Analysis length	50 s

Table 1. Laser and analytical parameters

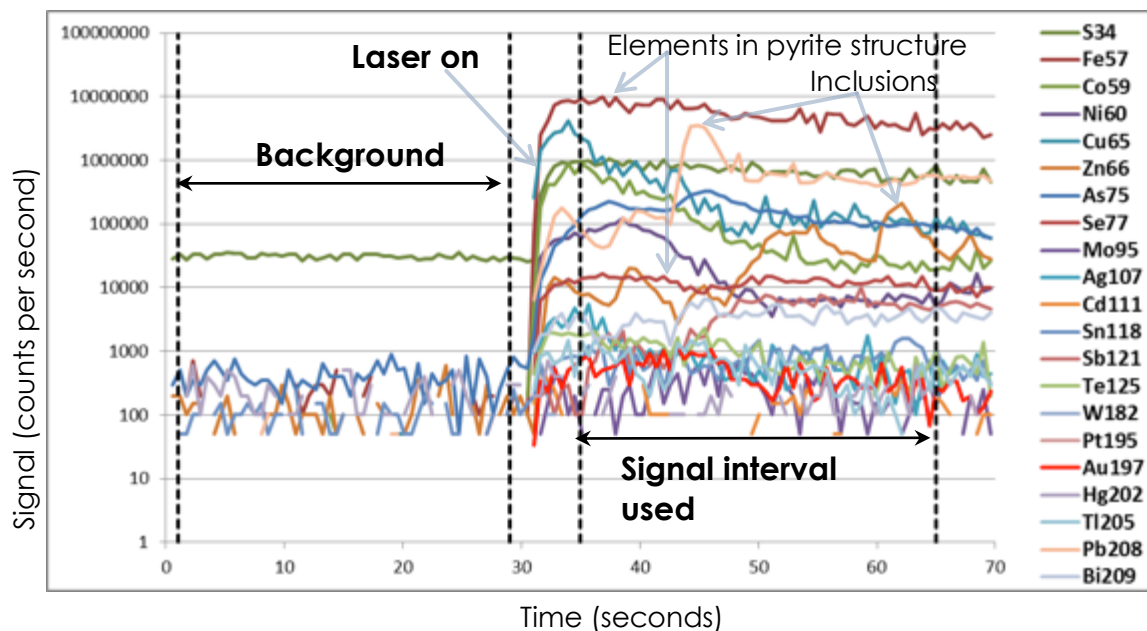


Figure 1. A time-resolved laser ablation signal for a pyrite analysis recorded on the ICP-MS (this example is not from the current project).

SAMPLES

PETROGRAPHY

Sample GRTD-039

Sample of exhibiting a wide variety of major sulphides and featuring pervasive dolomite and minor interstitial calcite. Sulfide component comprised of coarse, euhedral pyrite with chalcopyrite inclusions, large, euhedral chalcopyrite with bournite and late tennentite overgrowths supergene, covellite forms on the edge and in cracks of some grains.

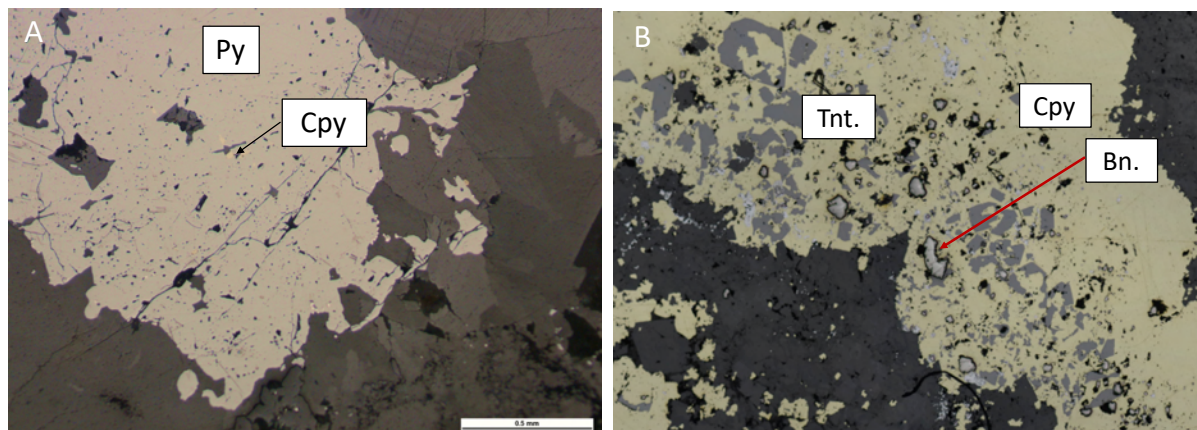


Figure 2. A – Euhedral- subhedral pyrite with Cpy inclusions and supergene covellite in cracks. B- Chalcopyrite with minor pyrite inclusions and bournite interspersed within the chalcopyrite. Tennantite overgrowth on Cpy.

Sample GRTD-040

Sample of oxidised Cu-ore, featuring pervasive dolomite and minor interstitial calcite. Sulfide component comprised exclusively of coarse, euhedral chalcopyrite with later, supergene, covellite forming on the edge and in cracks.

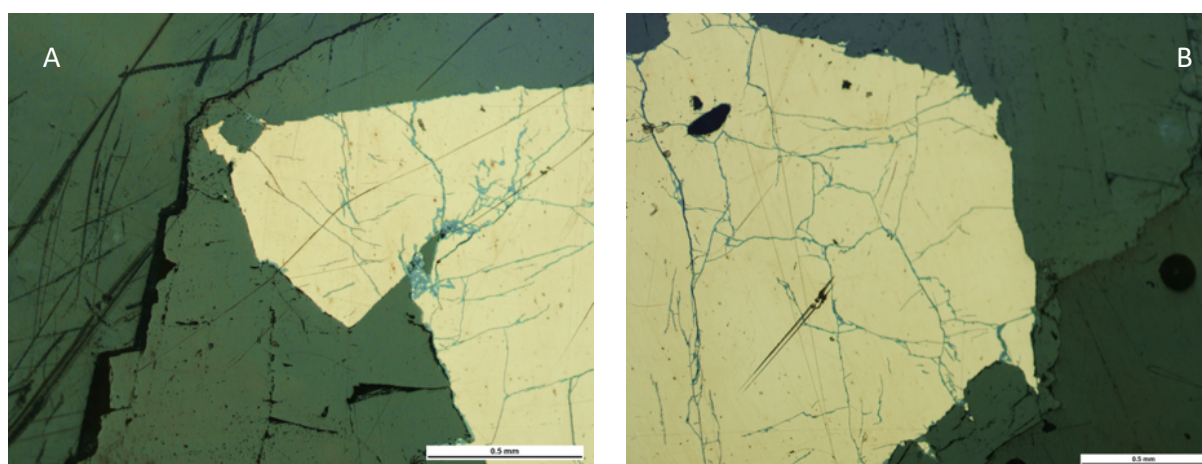


Figure 3. Examples of chalcopyrite with supergene covellite growth on rims and in cracks.

Sample GRTD-042a & Sample GRTD-042b

Heavily weathered sample of a carbonate vein with tennantite and Fe-oxides. Tennantite appears tarnished and is scattered in small clusters throughout the whole sample, therefore two mounts were made for this sample in order to gain enough material to analyze.

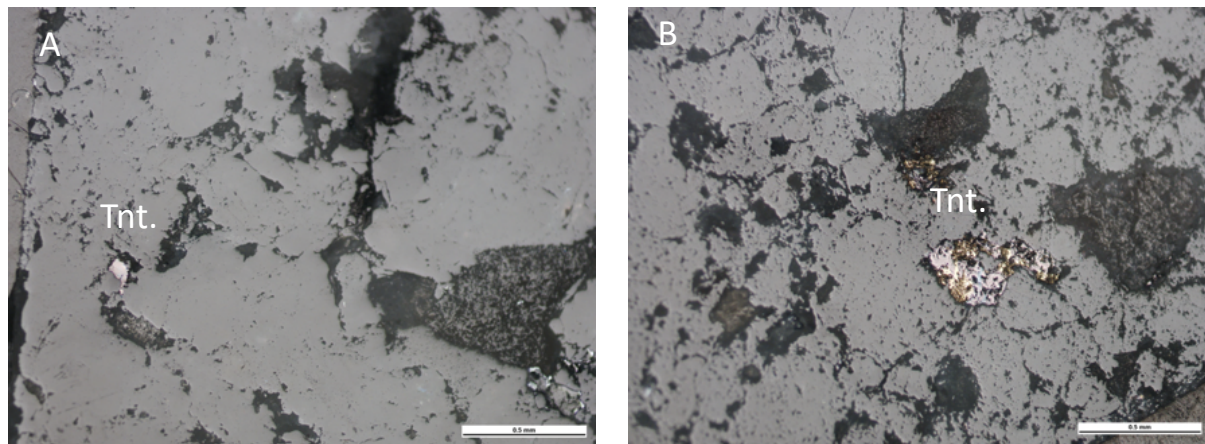


Figure 4. Tennantite clusters in a carbonate, with interstitial carbonate vein.

Sample GRTD-050

Heavily weathered sample of pervasively veined material with arsenopyrite and minor chalcopyrite. Well-developed arsenopyrite appears to postdate the minor chalcopyrite and does not contain any notable inclusions.

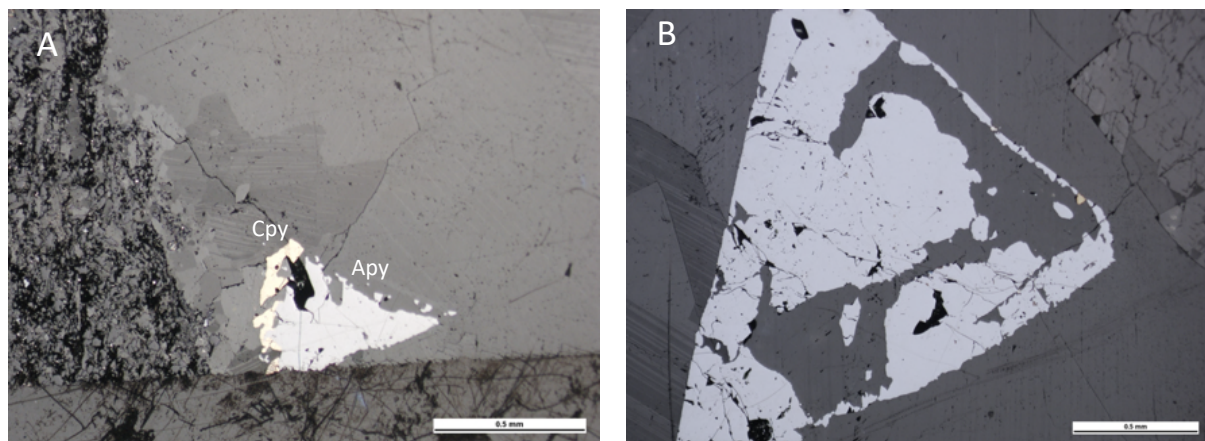


Figure 5. A- Euhedral arsenopyrite post-dating chalcopyrite in a quartz-carbonate vein. B- large euhedral arsenopyrite grain within a quartz-carbonate vein matrix.

Sample GRD-052

Sample of quartz-dolomite hosted sulphides. The main sulfide in this same was chalcopyrite. The chalcopyrite hosted a number of bournite inclusions, predominantly towards the edge of the mineral grain. Tennantite was also present, overgrowing the primary sulphides.

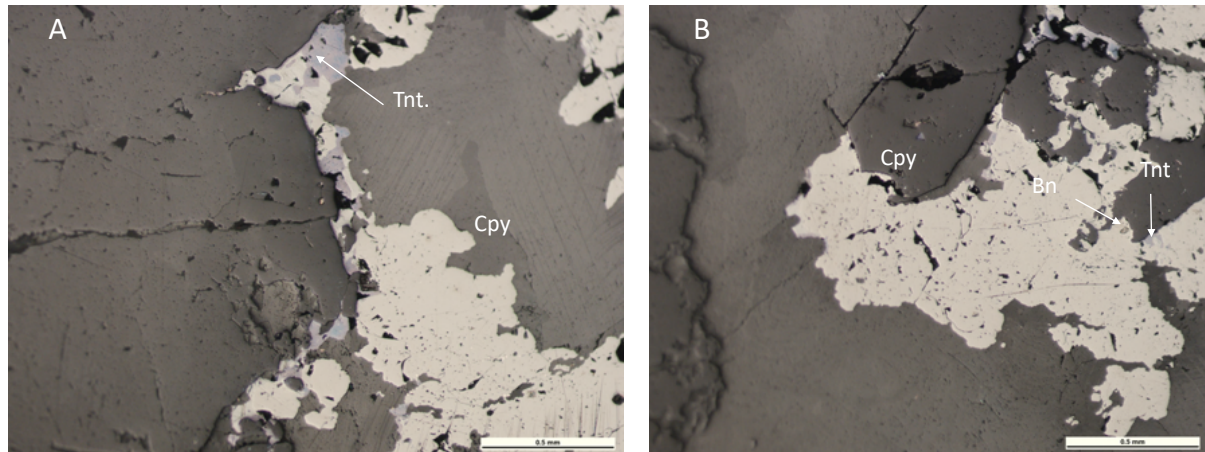


Figure 6. A- Chalcopyrite and with tennantite overgrowths. B- Chalcopyrite with bournite inclusions and tennantite overgrowths.

Sample GRD-055

Sample with clusters of chalcopyrite and tennantite in a dolomite calcite band with minor oxidation of some sulfide clusters.

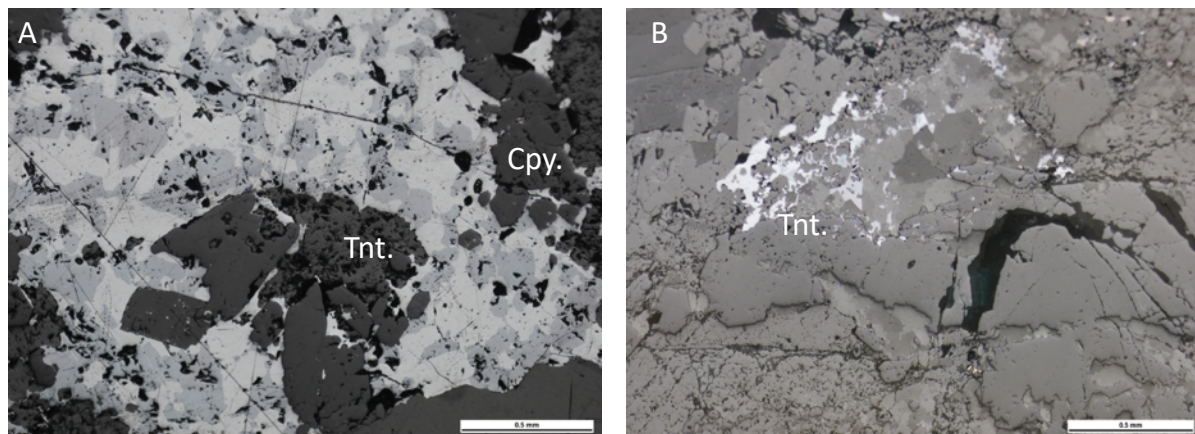


Figure 7. A- chalcopyrite cluster with subhedral tennantite overgrowths. B- Tennantite cluster in dolomite-calcite with minor Fe-oxidation.

Sample GRTD-059a & 59b

Clusters of chalcopyrite in a carbonate matrix. The main sulfide present is chalcopyrite with minor pyrite inclusions toward the edges of the grains and bournite inclusions throughout the chalcopyrite and likely synchronous. Tennantite overgrows the primary sulphides and a arsenopyrite-carbonate veinlet cross cuts the sample. The arsenopyrite displays a bladed texture, likely as a result of rapid cooling from a hydrothermal fluid.

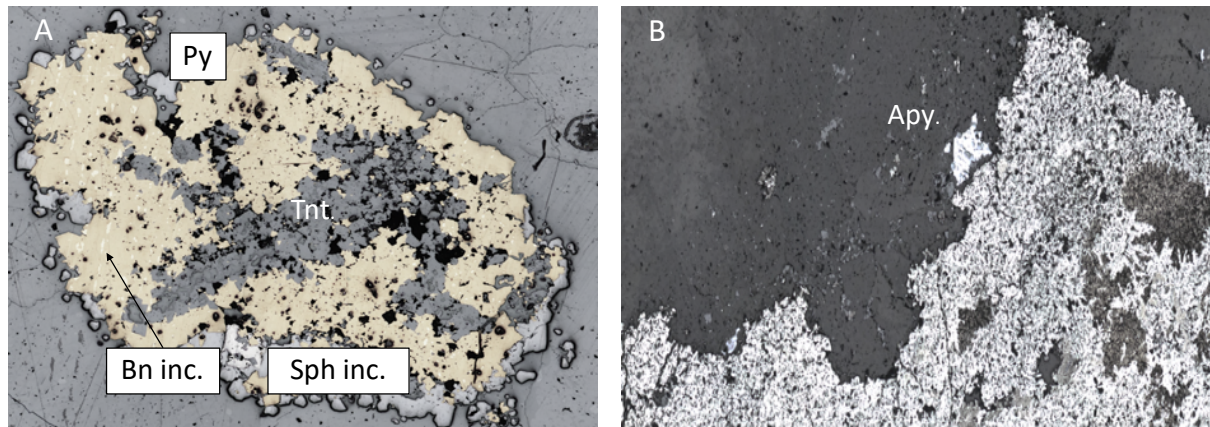


Figure 8. A – Chalcopyrite overprinting pyrite (py inclusions still visible in places) with bournite present throughout the chalcopyrite. Micro-inclusions of sphalerite are also present, see Fig.15

RESULTS

PARAGENESIS

The number of samples were limited, therefore a complete paragenesis cannot be achieved. However much work has been conducted previously on the deposit, including when access was available and therefor either proposed paragenesis from Duane (1998) (Fig.10) was used as a basis to inform the observations made.

Minerals	Time	
	Propyliti- zation Stage	Vein/ Replacement Stage
Pyrite	—————	
Chlorite	—————	
Clay ^a	—————	
Leucoxene	—————	
Ferroan-dolomite	— — — —	—————
Pitchblende		—
Brannerite		— ?
Coffinite (?)		— ?
Hematite		—
Tennantite		—
Chalcopyrite		—
Bornite/Chalcocite		—
Chalcocite/Stromeyerite/Wittichenite		—
Cinnabar/Native amalgam/Stromeryite		—
Covellite		Supergene
Malachite		Supergene
Azurite		Supergene
Secondary uranium minerals		Supergene

^a Both fuchsite and sericite have associated pitchblende

Figure 9. Paragenetic sequence for Gortdrum mineralization proposed by Duane, 1998.

Notably, the paragenesis does not mention Zn and Pb- bearing minerals that are present in the rest of the Irish Orefield. These minerals are present as small inclusions (see later section and Fig. 15) within the chalcopyrite. It is likely these are only resolvable on the scale at which the laser operates and likely are not visible during basic light microscopy.

Presented below is a revised mineral paragenesis, based upon the samples provided. There are two distinct As-bearing pyrite phases present, however they both appear to postdate main mineralization and cross cut it, therefore they have been grouped together. Pyrite appears to form early in the sequence, in agreement with Duane, 1998, however there are examples of it occurring with Cpy which is why it is inferred to be continuous during the main ore event. On the scale of the samples, the wider association of dolomite and calcite in sequence could not be ascertained, therefore the original paragenesis was used for these minerals.














Phases	Pre-Ore Stage	Early mineralization	Main Cu-Mineralization	Late (veining)	Supergene
Dolomite					
Calcite					
Pyrite					
Sphalerite					
Galena					
Chalcopyrite					
Bornite					
Tennentite					
Arsenopyrite					
Covellite					

Table 2. Paragenetic sequence for samples studied in this project, adapted from Duane, 1998. Note: Observations in red denote minerals that could not be placed in a greater paragenesis therefore are based upon that proposed by Duane, 1998.

TRACE ELEMENT ANALYSIS

Trace element analysis (via LA-ICP-MS) was conducted on each mineral present in each sample. While every effort was made to select useable material some analyses were discarded due to low yield or the presence of abundant micro- inclusions. Analyses were aimed at gathering an even distribution across the different minerals present (see below). Upon the data first being converted from counts per second to parts per million concentrations the data were plotted against the stoichiometric values of each mineral to ensure the right formulas for normalization were used.

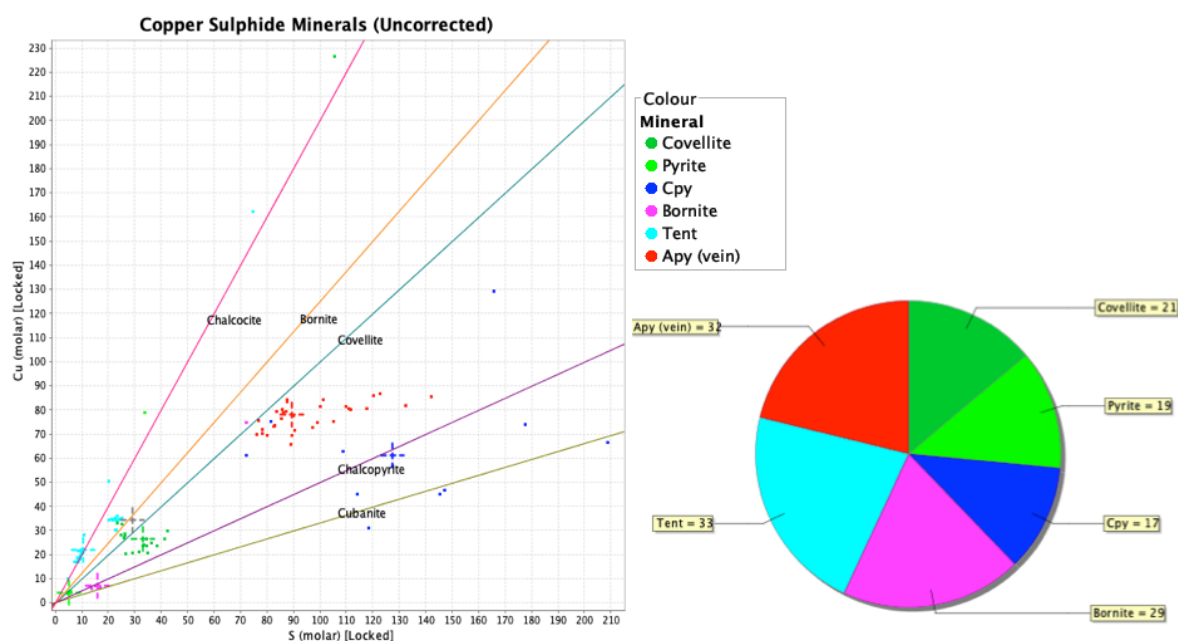


Figure 10. Distribution of spot analyses made across mineral type and raw data composition of the minerals analysed relative to stoichiometric compositions.

Pyrite composition:

In most pyrites As, Co, Ni, Ag, and Se are refractory, although inclusions of sphalerite or galena are present in some analyses; Cu and W also occur as inclusions or as discrete zones within the mineral with Ag spikes associated with galena inclusions. Au, Ag, Pt and Te contents are low, or below detection limit in some analyses.

Chalcopyrite composition:

Chalcopyrite is the main Ag- and Au-bearing phase analysed (5.6 ± 1 ppm Au; Appendix 1), which are refractory in nature within the mineral. However, the concentration of Ag and Au does vary between individual chalcopyrite analyses. Chalcopyrite also contains the highest values of Ni, Se, Zn, Pb and Te, the latter associated with Au and the Pb present as micro-inclusions of Ga and Sph, respectively. Nickel and cobalt are refractory within the mineral, as is Se, and Sb. Arsenic, Sn and Bi concentrations are variable between analyses but all tend to occur as discrete concentrations or clusters of micro-inclusions within the mineral and are often most commonly found toward the edge of the mineral rather than the centre.

Bournite composition:

Bournite tends to mirror the same element content as the chalcopyrite but they are present in much lower quantities. This may be due to the bournite always appearing as inclusions within the chalcopyrite, meaning that it had limited growth potential and therefore was limited in its ability to concentrate available trace elements.

Tennantite composition:

Tennantite is the main Bi-bearing phase analysed (300 ± 41 ppm Ag; Appendix 1), which is refractory in nature within the mineral. This phase also contains Cu, As, Se, Te and Ag

As-pyrite composition:

Arsenopyrite is present as a late stage veins in two samples, each with different textures. The two samples however do display very very similar trace element contents, suggesting they are both derived from a similar fluid composition. Arsenopyrite has variable Au and Te contents (av. 0.5 ± 0.2 ppm Au and 5 ± 2.9 ppm Te; Appendix 1). This appears to be concentrated more at the rims and/or clusters of micro-inclusions within the mineral. The exact distribution is not resolvable at the resolution used in the analysis. If it is the former then they may show association with Cpy previously analysed, in that it also appeared to have Au concentrated towards the edge of the grains. However a more detail comparison study would be required to investigate this fully. Lead, Cu Sb, Sn and W occur as small inclusions. Bismuth appears to concentrate as discrete zones within the mineral or as clusters of micro-inclusions (the exact distribution is not resolvable at the resolution used in the analysis). Nickel and Co are refractory in all samples analysed with this phase consistently containing some of the highest Co values of all phases analysed.

Covellite composition:

Supergene covellite contained Bi, Se, Te, Pb and Ag in high abundance, likely remobilised from the Cu-bearing minerals. Copper, Se, Co and Ni all appear to be refractory while Pb and Ag are likely associated together in micro-inclusions. It is understandable that Bi and Te are high in this phases as they are also present in higher concentrations towards the edge of the chalcopyrite grains where the covellite is forming, and presumably is being derived.

Element Associations and mineral paragenesis:

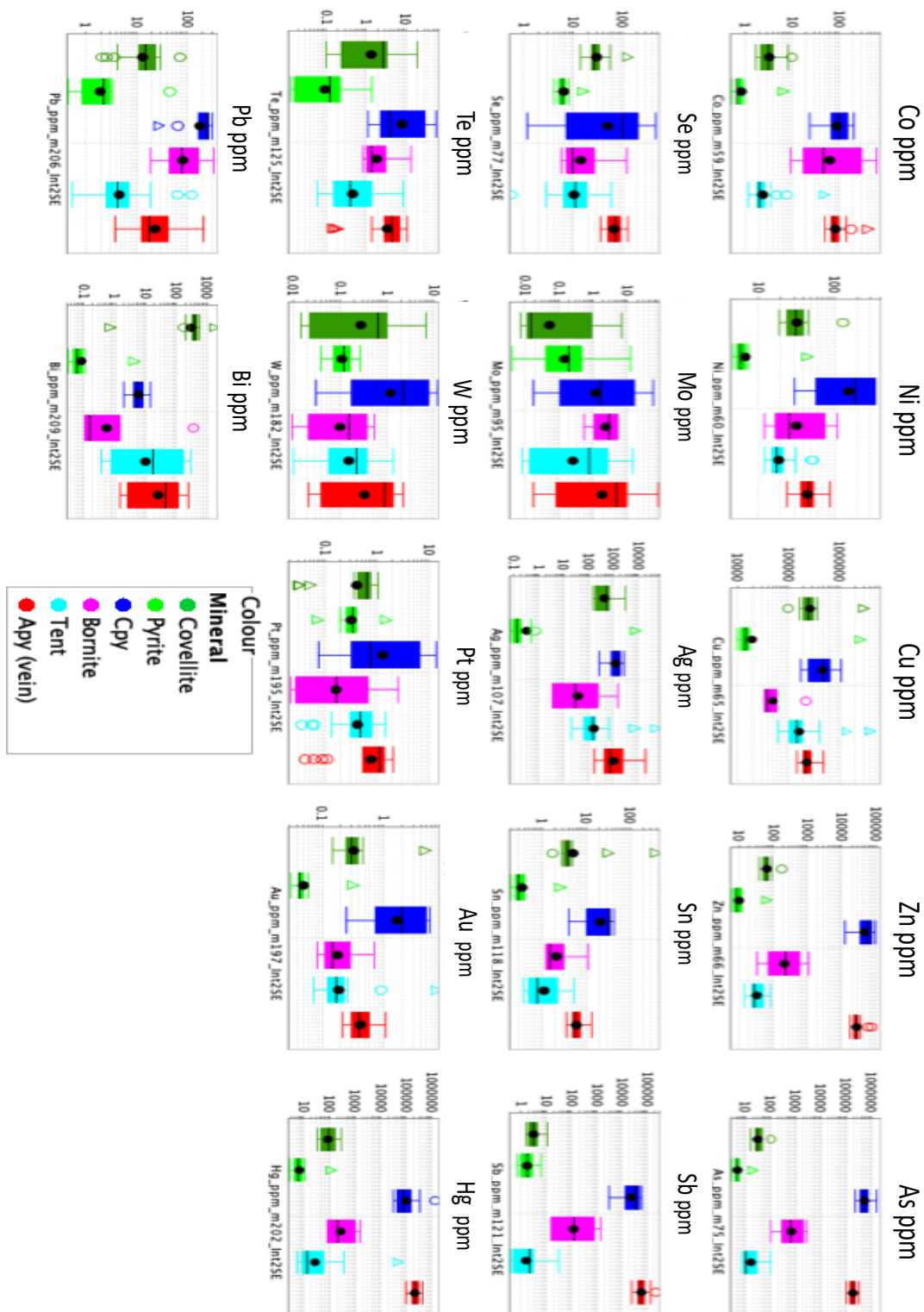


Figure 11. Distribution of trace elements relative to mineral phases. N.B it is likely the larger outlier reflect contributions from other mineral phases mixed with the analysed mineral or micro-inclusions.

Comparing the trace element content of each of the phases with respect to their interpreted paragenetic history suggests that the stabilization of chalcopyrite first incorporated much of the Cu, Zn, (Pb), As, Au, Ag, Te, and Sb in the system, while bournite mirrors these same elements associations they occur in lower concentrations. The earlier pyrite phase is trace element poor, with only Ni, Se and Co in notable concentrations. This is an interesting feature as typically pyrite tends to host a wide range of elements and is capable of doing so in high concentrations. Therefore, it suggests that pyrite forming at this time was not forming from a fluid rich in metals and that chalcopyrite was the main host for metals during formation. This observation is interesting as it could stand to reason that distal representations of Gortdrum may be expressed in metal-rich pyrite distal that forms towards the margins of the system where chalcopyrite may not be stable.

The textural evidence suggests that the arsenopyrite was the last in sequence to form and the trace element associations support this conclusion in that it has included all residual trace elements that were not incorporated into the chalcopyrite and elements that are particularly common in hydrothermal fluids.

The As, Sb and Sn help to also constrain the relative time of the mineral formation with respect to the mineralizing fluid(s) in that these elements are concentrated at the edge of the chalcopyrite. i.e. towards the later stages of growth, occur as small inclusions within the mineral, but appear to be widely dispersed throughout the Arsenopyrite. Furthermore, since the Au appears to also be concentrated towards the rim of the chalcopyrite, along with the previously mentioned elements, and doesn't not appear to be present in the associated bournite inclusions that are considered to be co-eval, this also may aid in identifying the period of peak gold concentration in the mineralizing process- i.e. towards the end of chalcopyrite formation and again, in minor amounts, during the hydrothermal arsenopyrite veining.

Chalcopyrite and pyrite are stable across a range of temperatures and sulfur fugacity, however the formation of arsenopyrite towards the end of the mineralization event would require an increase in sulfur fugacity or change in pH and temperature (Hall et al., 1987; Thomkins et al., 2006). Such changes could be a result of changes in the evolution of the fluid or the introduction of an additional sulfur source e.g. multiple rock types that may have interacted with the metal bearing fluid as it passed though. Additional isotopic work (i.e. S and Pb) would be required in order to strengthen or refute this hypothesis.






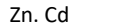
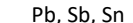
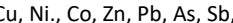

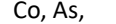
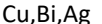
Phases	Pre-Ore Stage	Early mineralization	Main Cu-Mineralization	Late (veining)	Supergene
Dolomite					
Calcite					
Pyrite			 Fe, Cu, Ni, Se		
Sphalerite			 Zn, Cd		
Galena			 Pb, Sb, Sn		
Chalcopyrite			 Cu, Ni., Co, Zn, Pb, As, Sb, (Sn),Te, Ag, Au, Pt, Hg		
Bornite			 Cu, Ni., Co, Pb, As, Sb, Te, Ag,		
Tennentite				 Co, As, Hg, Se, Sb, Ag, Te	
Arsenopyrite					
Covellite					 Cu,Bi,Ag

Table 3. Paragenetic sequence for Gortdrum mineralization based upon this sample set with additions proposed by Duane, 1998 in red.

DISCRIMINATION PLOTS

It appears that arsenopyrite does not carry a large amount of economically important trace elements and tends to carry penalty elements (Hg, Sb, As) with Cu mineralizing pre-dating the arsenopyrite hydrothermal event. Therefore, discrimination between these minerals could prove useful in aiding understanding of prospectively and timing within the mineralizing system. A common way to apply this is with use of cross plots containing elements that vary as a result of different mineral phases or different events. Nickel vs Cobalt ratios are a common first-pass approach as Co:Ni ratios over 1 suggests excess Co which is typical feature of hydrothermal fluids, whereas increased nickel in sulphides is more common as a result of diagenetic and/or lower temperature fluids. The plot below shows that arsenopyrite likely represents a different fluid event, carrying a much more pronounced hydrothermal signature. This suggestion is supported by the textural evidence of blade arsenopyrite, typical of rapid cooling from hydrothermal fluids.

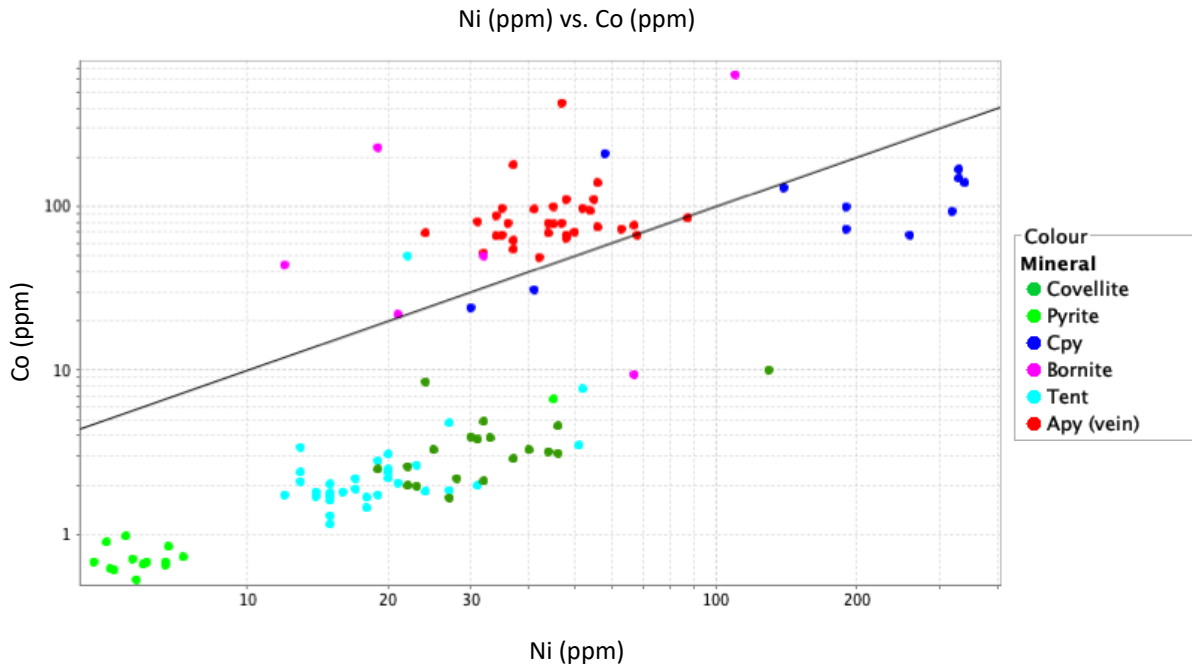


Figure 12. Ni vs Co plot for all minerals analysed.

The plot below employed a bespoke index calculation based upon the variance of elements between the chalcopyrite and arsenopyrite phases and used Bi as an additional discriminator as the arsenopyrite plotted higher in Bi as did the covellite with moderate values in the tennantite.

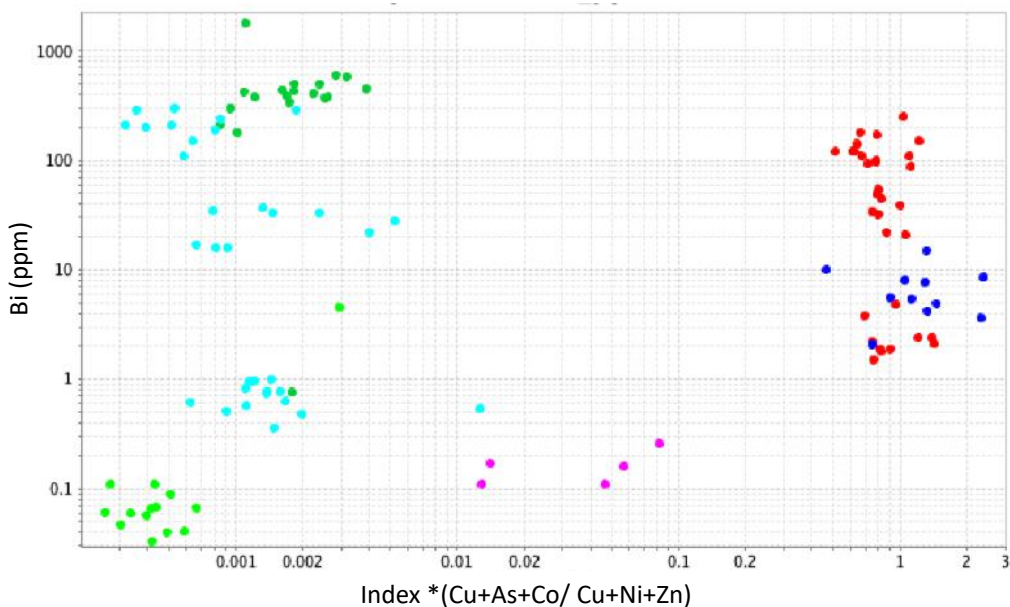


Figure 13. Bi vs Cu* index plot for all minerals analysed.

The plot below used the same index calculation but used Pb as an additional discriminator as it would be an element more easily quantified on various field portable analysis equipment.

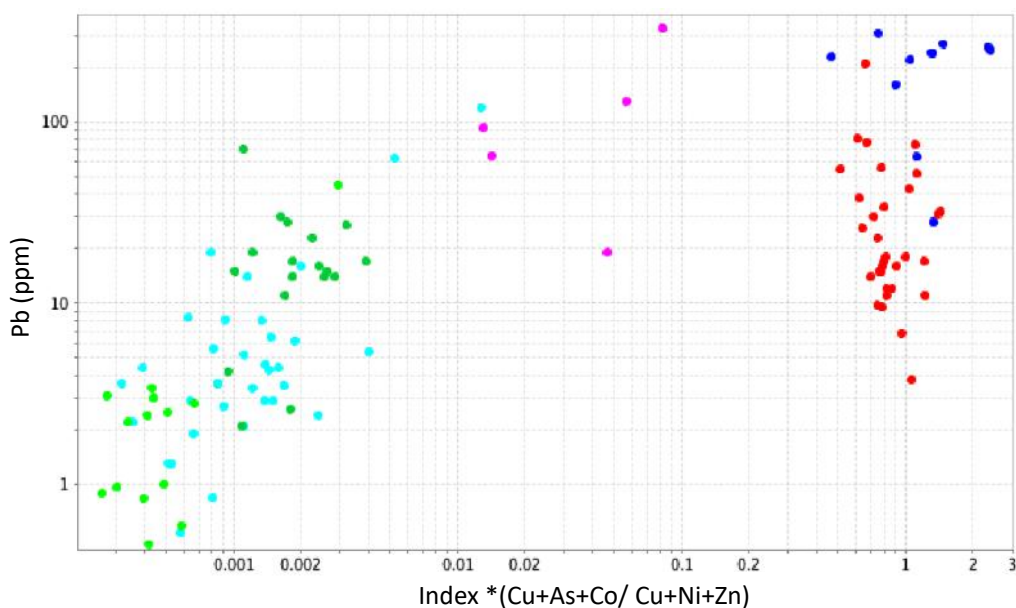


Figure 14. Pb vs Cu* index plot for all minerals analysed.

EXAMPLES OF ICP-MS OUTPUTS

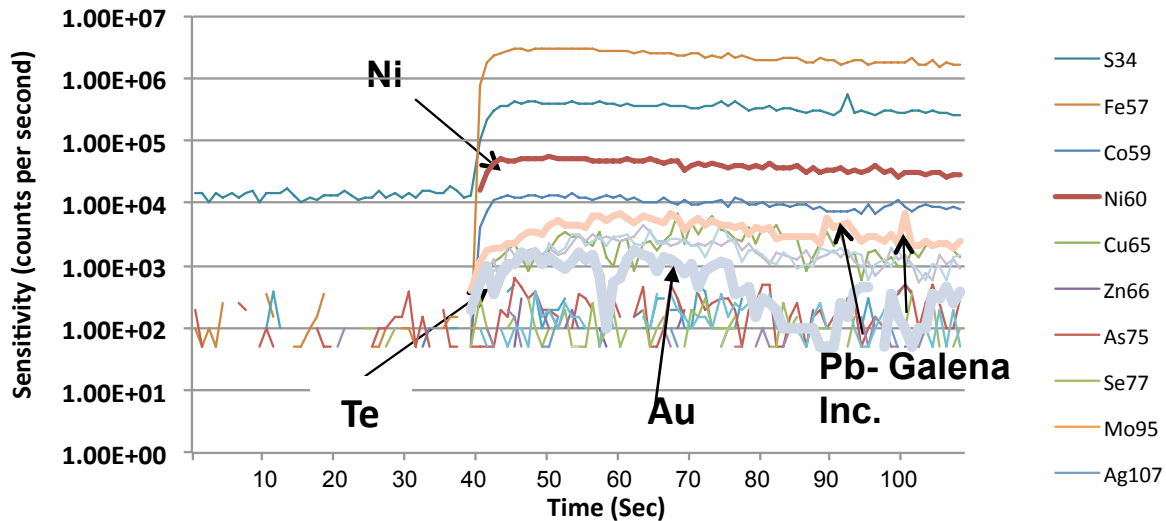


Figure 15. Example of chalcopyrite analysis with Au values higher towards the edge of the grain, Ni as refractory and minor galena inclusions.

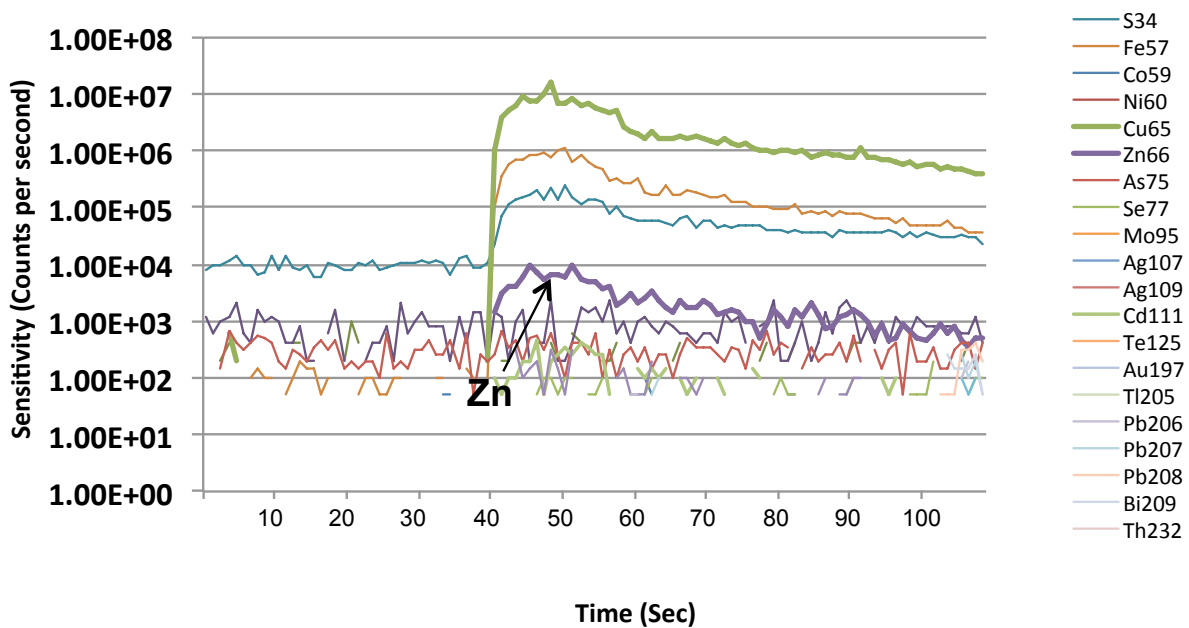


Figure 16. Example of chalcopyrite analysis with minor dispersed Zn as likely micro-inclusions.